

Use of Time-Frequency Analysis and Neural Networks for Mode Identification in a Wireless Software-Defined Radio Approach

Matteo Gandetto

Signal Processing and Telecommunication Group (SP&T), Biophysical and Electronic Engineering Department, University of Genoa, 16145 Genoa, Italy
Email: gandetto@dibe.unige.it

Marco Guainazzo

Signal Processing and Telecommunication Group (SP&T), Biophysical and Electronic Engineering Department, University of Genoa, 16145 Genoa, Italy
Email: guainazzo@dibe.unige.it

Carlo S. Regazzoni

Signal Processing and Telecommunication Group (SP&T), Biophysical and Electronic Engineering Department, University of Genoa, 16145 Genoa, Italy
Email: carlo@dibe.unige.it

Received 4 September 2003; Revised 8 June 2004

The use of time-frequency distributions is proposed as a nonlinear signal processing technique that is combined with a pattern recognition approach to identify superimposed transmission modes in a reconfigurable wireless terminal based on software-defined radio techniques. In particular, a software-defined radio receiver is described aiming at the identification of two coexistent communication modes: frequency hopping code division multiple access and direct sequence code division multiple access. As a case study, two standards, based on the previous modes and operating in the same band (industrial, scientific, and medical), are considered: IEEE WLAN 802.11b (direct sequence) and Bluetooth (frequency hopping). Neural classifiers are used to obtain identification results. A comparison between two different neural classifiers is made in terms of relative error frequency.

Keywords and phrases: mode identification, software-defined radio, frequency hopping code division multiple access, direct sequence code division multiple access, time-frequency analysis, pattern recognition.

1. INTRODUCTION

The ideal software radio (SR) [1] can accommodate all existing bands and modes in a host terminal or, more generally, in a platform. Toward this end, SR defines all radio frequency (RF) aspects (filtering, access methods, etc.) and transmission/reception layer functions (modulation, coding, etc.) in software terms to support multimode, multiband communications. In general, SR can be applied to base stations (BSs) [2] or to user terminals (UTs). SR-based transceivers are characterized by high levels of adaptability, flexibility, and reconfiguration.

The ideal SR leads to a revolution in the design of a transmitter/receiver terminal (if used in a BS or UT) with respect to the conventional radio devices based on the classical heterodyne schemes [3]. The analogical part of an SR-based

device is very reduced (only the antenna, the low noise amplifier (LNA)), and it should be designed to receive all existing available modes and not a particular one [4]. The D/A and A/D conversion processes move closer to the antenna. In the case of reception, the signals associated with all communication modes present in the radio environment are first sampled (by A/D) at high frequency and then represented in a digital format, whereas, in the case of transmission, D/A converts all generating modes for further transmission. The entire baseband computation is performed with digital signal processing (SP) techniques and fully software defined [4]. The ideal SR is the target that should be reached to realize future generation wireless terminals. Unfortunately, with the current technology (hardware and software), this target is difficult to attain. An SR-based transceiver, like that described above, is not yet feasible. For example, it is not possible to

design a wideband receiving antenna to receive all multiband modes or to design D/A and A/D converters with sufficient dynamic range, quantization, and sampling frequency, as required in SR applications [5]. On the other hand, from a software point of view, the design of flexible procedures able to satisfy the constraints of a real-time communication, at high frequency, and with sufficient computational capabilities, is not yet possible.

Therefore, starting from the SR philosophy and trying to reach its targets with current technology, the actual solution for realizing SR-based transceivers is to use an RF conversion stage that brings a received signal to intermediate frequency (IF) to allow the use of commercial D/A and A/D converters [1]. To support multiband communications, antenna arrays [6] or different RF stages can be employed [7]. This solution is known as software-defined radio (SDR) and can be defined as a radio that can receive and transmit a large number of modes in different bands. The SDR approach is a great evolution based on the programmable digital radio (PDR) paradigm, which consists in a radio fully programmable in baseband stage by employing digital signal processors (DSPs). More precisely, according to the technical definition of the SDR forum, "SDR is a collection of hardware and software technologies that enable reconfigurable system architectures for wireless networks and user terminals" (www.sdrforum.org).

In the SR domain, it is worth mentioning the cognitive radio (CR) [8]. This paradigm extends the concept of SR to allow the design of a radio device (based on SR) that understands the user's communication needs, and provides the user with the most suitable radio services within a particular context. This new evolution offers reasoning radio with conscious capabilities based on the SR paradigm [9].

In this scenario, the present paper describes the receiving part of an SDR-based UT, in particular, its physical layer is highlighted. As explained before, in the design of an SR terminal, many problems arise from both the hardware and software points of view [1]. However, some issues also concern the context of the SP domain for SR, in particular, for SDR-based devices. One of the most important open issues in SP is the objective of this work, that is, mode identification (MI) [10]. More precisely, an SDR receiver should be able to monitor the radio channel over a certain frequency range (ideally, the widest possible) and classify all possible communication modes by applying digital SP techniques directly to the sampled version of incoming electromagnetic signals provided by A/D. The solution of demodulating in parallel a large set of transmission modes, the so-called "velcro approach," is infeasible at the receiver according to SR vision, and introduces a high level of complexity into the hardware receiver structure. A more suitable solution, explored in this paper, is to try to identify, at a lower abstraction level, multiple transmission modes directly from the sampled version of a signal. By this procedure, the device classifies the standards available in the environment before decoding and extracting the modulated information contained in the signal.

Once the available mode is identified, an SR terminal should set up all necessary procedures to support it: if the

software modules (which perform the receiving operations) are present in the terminal, after A/D conversion, baseband SP procedures, like demodulation, decoding, and so forth, follow; otherwise, software libraries have to be downloaded from the network [1]. The MI problem is faced here in the context of SDR because it is the available technology up to now used to realize the SR paradigm. However, this concept is a fundamental and integrating part of SR and CR because it allows one to support multimode and multiband communications according to SR.

In general, MI can be blind or assisted [10], and modes can be superimposed in the same band or not. In the blind approach, no previous information about the modes present in the monitored radio environment are available at the UT which has to recognize the modes directly from the received signals. In the case of assisted identification, the UT has previous information or receives it from the network. This is also known as network-aided identification. In this work, the first kind of MI will be addressed considering superimposed modes.

The state of the art provides the following methods. Energy detection [11] is a common procedure with a low processing load to recognize the presence or absence of a signal. Unfortunately, when signals temporally overlap on the same bandwidth, energy detection can be insufficient to discriminate the mode. Moreover, the information provided by energy detection cannot be enough to take further steps, for example, in the direction of modulation recognition. A recent work [12] presents the use of a radial basis function (RBF) neural network for a power spectral density estimation to identify the communication standard. No superposition of signals is considered and different RF stages are employed. The European project TRUST (European research project transparent ubiquitous terminal) presents an MI system for GSM and UMTS standards [10].

In this paper, a nonlinear SP method is proposed; namely, time-frequency (TF) analysis [13] combined with a pattern recognition approach to solve the problem of MI in the context of a specific signal superposition. In this case, the identification process is more difficult because modes interfere among them, and the methods offered by the state of the art cannot be used. TF analysis allows one to extract important features, used as input to the classifier to establish which kind of mode is actually available in the radio environment. Two TF distributions, the Wigner-Ville (WV) and the Choi-Williams (CW) transforms [13], are applied. Moreover, two kinds of neural classifiers are adopted: a simple feedforward network based on back propagation and a support vector machine (SVM), both using supervised training [14, 15]. Results in terms of relative frequency of classification errors are presented and discussed. As a case study, two standards are considered: WLAN 802.11b [16] and Bluetooth [17]. The choice of these two standards stems from three factors: first, they are based on DS-CDMA and FH-CDMA, the chosen modes; second, they use the same bandwidth (Industrial Scientific Medical (ISM) Band) with the possibility of designing a unique RF conversion stage, as ideally required for an SDR platform [1]; third, the growing interest in them

TABLE 1: Physical level characteristics of the Bluetooth and IEEE 802.11b standards.

Characteristic	BLUETOOTH	WLAN
Air interface	FH-CDMA $t_{\text{hop}} = 1/1600$	DS-CDMA
Modulation	GMSK	CCK-DQPSK
Channels	82	13
Max coverage	max 10 m	max 100
Bandwidth	1 MHz	22 MHz
Tx power	1 mW	25 mW

on the market for their wireless connectivity, especially for communications in the coexistent environment [18].

The paper is organized as follows: in Section 2, the problem statement explaining the reason for using an MI module is presented. In Section 3, the necessity for TF analysis is discussed. The proposed method and its subparts are investigated in Section 4. Numerical results are reported in Section 5 and conclusions are drawn in Section 6.

2. PROBLEM STATEMENT

In this paper, the problem addressed is the identification of spread spectrum (SS) modes, namely, DS-CDMA and FH-CDMA. The problem concerns the presence of a user able to move without constraints in an indoor environment and provided with a wireless SDR-based receiver. In particular, in this scenario, two wireless standards using SS modes and superimposed in the same bandwidth at 2.4 GHz are considered: IEEE 802.11b and Bluetooth [16, 17]. As explained above, they are employed for transmission the ISM band from 2.4 GHz to 2.4835 GHz. A single IEEE 802.11b channel uses 22 MHz for transmission [16], whereas Bluetooth uses the whole ISM bandwidth employing 79 frequency hops with a bandwidth equal to 1 MHz [17]. Other basic characteristics of the two standards are presented in Table 1.

In this preliminary study, the presence of other SDR UT receivers or conventional WLAN or BT devices is not considered. A downlink scenario where SDR-based receivers try to identify the available modes in the radio environment is addressed. The user's device is regarded as an SDR device provided with a high level of reconfigurability and sufficient processing capabilities to recognize and decode all the modes. The classical procedure of receiving the available modes separately is not applied here as we aim to limit unnecessary computational operations, in order to minimize the hardware redundancy in the receiver. In particular, if the problem was considered from a scalable and complete SR point of view, the number of standards should have been the largest; therefore, the necessary time and resources to perform a serial or parallel reception would sharply increase.

The above considerations suggest the use of an MI module: this tool should aim at the classification of available stan-

dards in the wireless environment without the complete reception and decoding of a signal. This involves a shorter recognition time, hence less use of terminal resources for these tasks; moreover, the classification of modes is not implemented directly in the receiver. As consequence, a very modular view of the device can be foreseen to meet SR requirements (www.sdrforum.org). These points are of major importance in the SR world, in which the device should recognize, in the shortest possible time, the modes available and realize as fast as possible if the classified standards are unavailable inside itself and also realize the libraries and software module downloads needed from the network.

3. WHY TIME-FREQUENCY ANALYSIS FOR MODE IDENTIFICATION?

In this paper, the use of TF analysis for MI by an SDR receiver is proposed and discussed. TF methods are powerful nonlinear SP tools that can be employed for analysis of non-stationary signals and in other different applications [19].

In this case, TF allows one to use a compact and robust signal representation. By using TF, signals can be represented in two dimensions: time and frequency. Therefore, TF methods potentially provide a higher discriminating power for signal representation. In particular, such representation is quite useful for SR, especially in the case of multimode superimposed communications. The use of TF for MI allows us to apply an adaptive reception strategy, in particular, to face signal superposition in the same band. In this context, a coexistent radio environment is presented where Bluetooth can interfere with WLAN and vice versa. The use of time and frequency analysis allows one to identify the presence of the two standards at a particular time instant and at a given frequency. An adaptive receiver provided with such information could use it to cancel the reciprocal interference of the two modes in an intelligent way, thus making it possible to design an adaptive interference suppression tool for different standards. This should allow better performances in the receiver expressed in terms of error probabilities. Such a result could be attractive in an SR receiver, as minimization of error probabilities on a larger set of transmission modes could be simultaneously obtained.

In the cases of IEEE 802.11b and Bluetooth, methods for decreasing mutual interference are currently under development, for example, use of adaptive frequency hopping transmission [20]. However, these topics will not be addressed in the present paper.

In general, to perform identification other features could be employed instead of those obtained by TF analysis, for example, features related to a received signal, like received signal strength (RSS). The main approach to obtaining RSS is to apply filters for extracting power to a limited bandwidth in two ways [11]: a single filter with a sliding window that examines the entire bandwidth [11] or a bank of filters centered on portions of the bandwidth [11]. However, when RSS is used for MI, some problems may arise, especially in the case of multimode communications with band superposition. In an SR scenario, some signals can be strongly nonstationary and

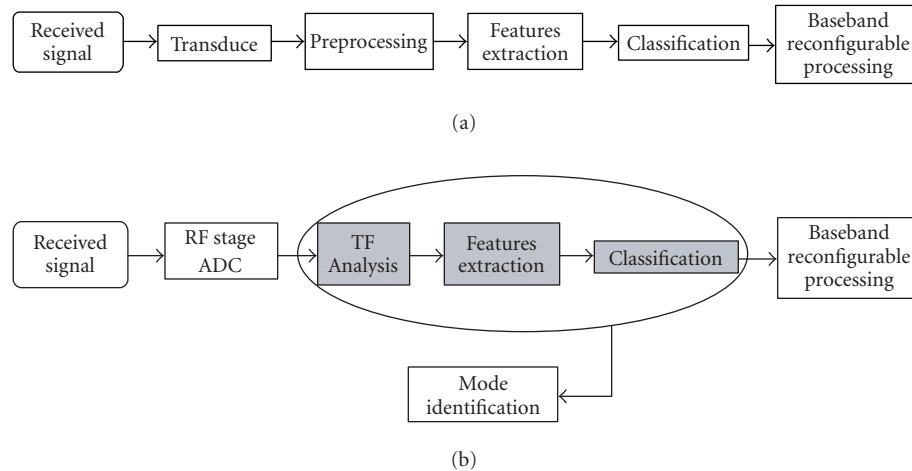


FIGURE 1: A general classification scheme and the proposed method for mode identification.

their occupied bandwidth can considerably vary over time. Therefore, filter design is more complex to realize, and the filter structure should take into account the nonstationary nature of signals.

Moreover, in the case of signals with equal RSS, identification may become critical. There might be no possibility of discriminating signals in a correct way, and an adaptive reception, like that presented above, may not be achieved. For example, in the case under investigation, from Table 1 it is possible to note different transmission powers for the two standards. However, due to the channel propagation model and the presence of path loss effects during transmission over a real channel, it might be possible to observe received signals with equal RSS. In this case, the RSS feature is not useful for MI.

Another great advantage of TF over other features, like RSS, for MI is the independence of the communication modes. This is quite important from the receiver design point of view. For example, when employing filters for extracting RSS, they should be matched to the signal to be detected, or the signal shape should be known. In the case of TF analysis, the latter constraint must not be fulfilled. TF provides a signal description even when no a priori knowledge of the signal shape is available. Therefore, the receiver structure based on TF methods for identification can be more modular and flexible in the presence of a multistandard environment, as compared with other methods. This can be a good attribute for an SR receiver. Moreover, if the bandwidth to be monitored is variable and a standard is added, the number of filters to be used can be different. This fact introduces into the receiver structure a hardware redundancy that, in the case of an SR device, should be avoided. To sum up, the use of TF tools for MI in a multistandard environment, especially in the case of signals superposition, is better than the use of other features. TF tools allow one:

(i) to design a flexible/modular SR receiver structure;

- (ii) to be independent of particular transmission modes;
- (iii) to obtain a higher discriminating power and a more effective signal representation;
- (iv) to use adaptive reception techniques.

A drawback of using TF analysis is computational complexity. However, in the field of hardware structures, chips to compute TF are being developed also for real-time applications [21, 22, 23, 24, 25, 26].

4. PROPOSED METHOD FOR MODE IDENTIFICATION

The proposed approach to performing MI is based on the following three main tools: (1) a TF tool, which computes the TF transform; (2) a feature extractor, which derives the main characteristics from a signal; (3) a classifier, which discriminates different standards.

A general classification system (Figure 1a) is composed of various modules. In the proposed method, each module can be mapped into the corresponding general block, as indicated in Figure 1b. In particular, after the RF stage and A/D conversion, the received signal is processed by a TF block. This block provides a TF representation (distribution) where the two modes (DS and FH) are well defined in the TF plane (Figure 2). A TF distribution is obtained from the TF block, where each element represents the TF value in the TF plane. Toward this end, the received signal is observed in a window multiple of the time T which is the sample time chosen on the basis of the standards' characteristics [16, 17]. This window has been designed to include 10 Bluetooth frequency hops (Bluetooth FH employs 1600 hops/s on 79 frequencies [17]). At the same time, the IEEE 802.11b DS CDMA signal is also present with its frequencies inside the window. The features obtained by the TF block are given to the classification module to identify the mode available.

In the following sections, each part of the scheme depicted in Figure 1b will be explained.

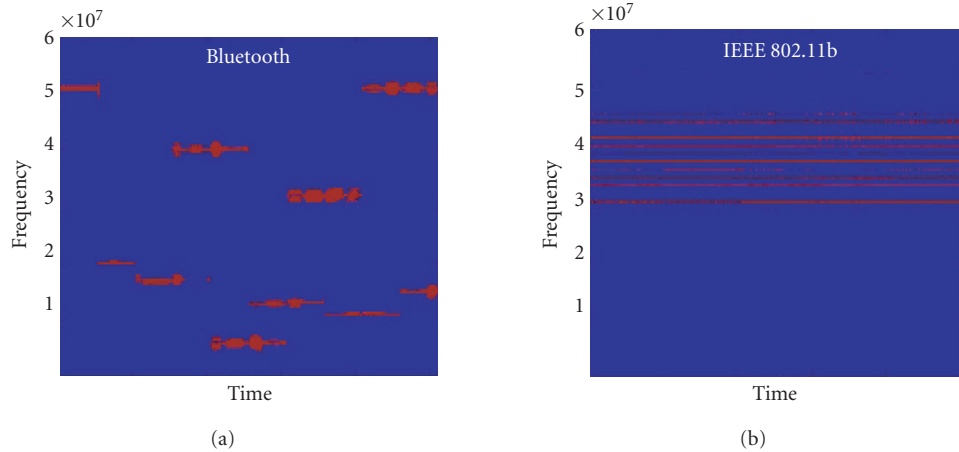


FIGURE 2: Time-frequency transforms of the two standards: (a) Bluetooth, (b) IEEE 802.11b.

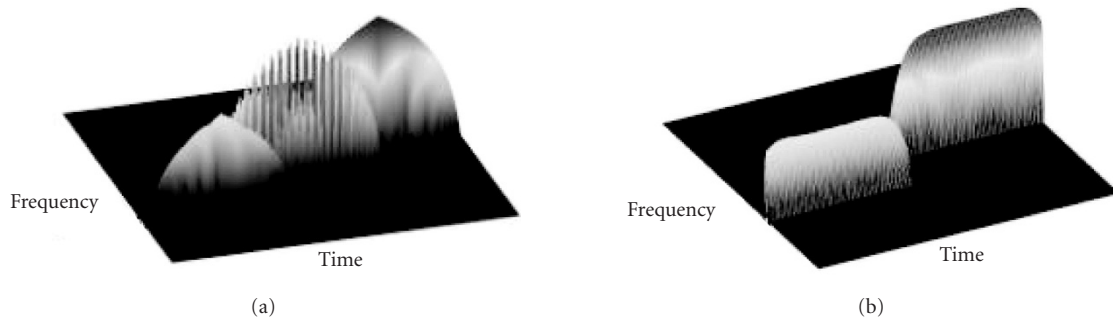


FIGURE 3: (a) Wigner distribution and (b) Choi-Williams distribution of an FH signal.

4.1. Time-frequency distribution

Two kinds of TF distributions are used: the WV distribution [13] and the CW distribution [27]. Both have advantages and disadvantages as explained below.

The WV distribution is the prototype for all TF transforms, and is the most widely used and the most important. Its optimal performances can be obtained for monodimensional signals, whereas multicomponent signals suffer from the presence of cross-terms (Figure 3a). According to the distribution profile for any signal of fixed length and moving on the time axis, the WV transform of a signal $s(t)$ increases up to the middle of the time window, then it decreases. Such a behavior produces a typical shape. This transform presents a low computational complexity, which is a suitable feature for real-time usage.

The Wigner distribution is given by the following expression [13]:

$$W(t, f) = \frac{1}{2\pi} \int s^* \left(t - \frac{1}{2}\tau \right) s \left(t + \frac{1}{2}\tau \right) e^{-j\tau 2\pi f t} d\tau. \quad (1)$$

The second transform, namely, the CW distribution, thanks

to its exponential kernel, reduces interference effects, thus providing a better and cleaner visualization of signals in the TF plane. Unfortunately, this improvement results in higher computational complexity. Another remarkable difference, as compared with the WV transform, is the profile of the signal distribution: the profile is not sharp but flat and this gives more precise estimates of the distribution borders.

The CW distribution is given by the following expression [27]:

$$W_{CW}(t, f) = \int e^{-j2\pi f t} \int \sqrt{\frac{\sigma}{4\pi\tau^2}} e^{-\sigma(\mu-t)^2/4\tau^2} \times s \left(\mu + \frac{\tau}{2} \right) s^* \left(\mu - \frac{\tau}{2} \right) d\mu d\tau, \quad (2)$$

where σ is a factor controlling the suppression of cross-terms and the frequency resolution. $W_{CW}(t, f)$ becomes the WV distribution when $\sigma \rightarrow \infty$. The integral ranges from $-\infty$ to ∞ and, in our case, $s(t)$ is the received signal.

The choice of the distribution for the preprocessing task must meet the following requirements:

- (i) representing a signal in an explicit and robust way;
- (ii) obtaining such a result by a low computational load.

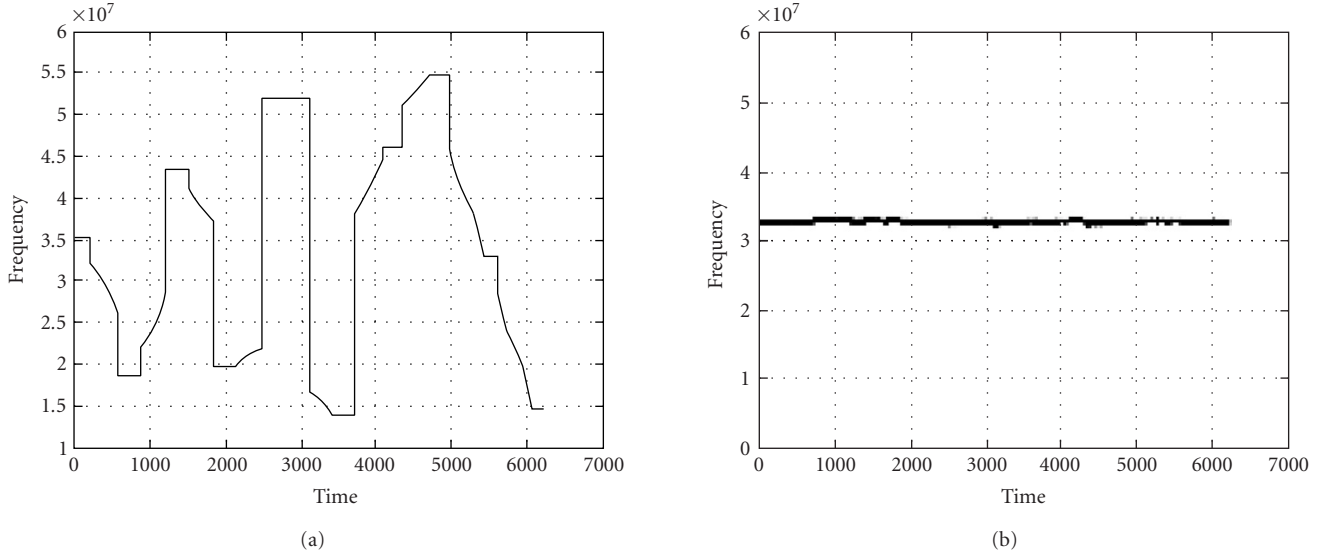


FIGURE 4: Examples of the first-order conditional moments, namely the instantaneous frequency, in the cases of (a) Bluetooth (frequency hopping) and (b) IEEE 802.11b (DS-CDMA).

The first requirement is satisfied more directly by the CW transform thanks to its exponential kernel, as explained above; on the other hand, the WV transform requires a lower computational load thanks to its simpler formula, an important feature in real-time usage.

In an MI task, the WV transform yields worse results than the ones achieved by the CW transform. Moreover, the problem of obtaining the first-order conditional moment by the WV distribution lies in the fact that it can take on negative values that are not physically correct. In the literature, one can find some TF distributions defined to obtain only positive values [28] of that parameter. In our case, just to simplify the computation, the Janssen method has been applied to the distribution [29], and positive values have been obtained by the WV distribution.

4.2. Features extraction

From the TF matrix, computed by either the WV transform or the CW transform, it is possible to extract the features of a received signal. Two features are studied in this paper:

- (i) the standard deviation of the instantaneous frequency;
- (ii) the maximum duration of a signal.

To obtain the first feature from a given TF distribution $P(t, \omega)$, the first conditional moment of the frequency is computed as [13]

$$\langle \omega \rangle_t = \frac{1}{P(t)} \int \omega P(t, \omega) d\omega, \quad (3)$$

where $P(t)$ is the time distribution and the integral ranges from $-\infty$ to ∞ . $\langle \omega \rangle_t$ is the average frequency at a particular time t and, most important, is considered as the instantaneous frequency [13]. So, if a signal is regarded as a generic bandpass signal composed of the amplitude component and

the phase component [13],

$$s(t) = A(t)e^{j\varphi(t)}, \quad (4)$$

its instantaneous frequency ω_i is

$$\omega_i = \varphi'(t) = \langle \omega \rangle_t. \quad (5)$$

From this parameter the first feature is obtained, namely, the standard deviation of the first-order conditional moment,

$$\text{std}(\omega_i) = \left(\frac{1}{T} \sum_{t=1}^T (\omega_i - \bar{\omega}_i)^2 \right)^{1/2}, \quad (6)$$

where $\bar{\omega}_i$ is the mean value of ω_i given by

$$\bar{\omega}_i = \frac{1}{T} \sum_{t=1}^T \omega_i. \quad (7)$$

This parameter is computed on a time window T longer than the time hopping period of the Bluetooth signal. From Figure 4, one can see that T has been chosen such as to obtain a low value of $\text{std}(\omega_i)$ when the first conditional moment is quite constant, as in the case of DS (IEEE 802.11b), whereas $\text{std}(\omega_i)$ takes on large values when the spectrum is strongly variable in time, as in the case of FH (Bluetooth).

The second feature is obtained on the basis of the following considerations. In the case of DS, frequency components are continuous in time for a duration that depends on the length of the time observation window T used to compute the distribution (see Figure 2b). Instead, for FH signals, discontinuities in time can be observed that are due to the presence of different frequency hops (see Figure 2a). Therefore, it is possible to obtain an empirical discriminating feature dependent on the time duration of the signal considered. To derive such data, the following operations are performed.

- (1) From the chosen transform, a binary TF matrix $P_{\text{bin}}(t, f)$ is obtained by thresholding the real-valued TF transform. The values of this matrix represent the presence (elements equal to 1) or the absence (elements equal to 0) of signals at a given time t and at a given frequency f .
- (2) The threshold has been chosen in an empirical way. After a trial and test procedure, its value has been chosen as the mean value of the original TF matrix.
- (3) Once $P_{\text{bin}}(t, f)$ has been obtained, the elements of each row of this matrix are summed up to derive the time durations of the signal components at a certain frequency.

These operations yield different values for each row of the TF matrix according to a run-length measurement scheme. The feature to be presented to the classifier has been chosen as the maximum value in such a set, that is,

$$T_M = \max \{T(\omega)\}, \quad (8)$$

where

$$T(\omega) = \sum_t P_{\text{bin}}(t, \omega), \quad (9)$$

where the summation is done over the entire length of the window where the distribution is computed.

4.3. Choice of the classifier

A multiple-hypothesis test has been carried out. In particular, four classes have been studied.

- (1) Class H0: presence of additive white gaussian noise (AWGN). This class will be denoted by "Noise."
- (2) Class H1: presence of WLAN signal with AWGN and multipath fading. It will be denoted by "WLAN."
- (3) Class H2: presence of Bluetooth signal with AWGN and multipath fading. It will be denoted by "Bluetooth."
- (4) Class H3: presence of both types of signals with AWGN and multipath fading. It will be denoted by "WLAN + Bluetooth."

The data extracted are dependent on the user's distance from the Bluetooth or the IEEE 802.11b BS. As a consequence, the classes, except Noise, move in the features plane according to the user's movement. In Figure 5, an example of the WLAN + Bluetooth class is given for a moving user. The first effect of this peculiarity is that a different linear classifier would be necessary for each user position. This solution is too complex and unfeasible. Therefore, a pattern recognition approach using neural classifiers has been chosen. With this technique, a theoretical model of experimental distribution is not necessary, thus the problem of modeling the probability density function (PDF) of each feature is avoided. Then, the classifier is the same for any location, being completely uncorrelated with the user's movements, and the analysis has been made for different positions with respect to the signal source, as will be explained in the next section.

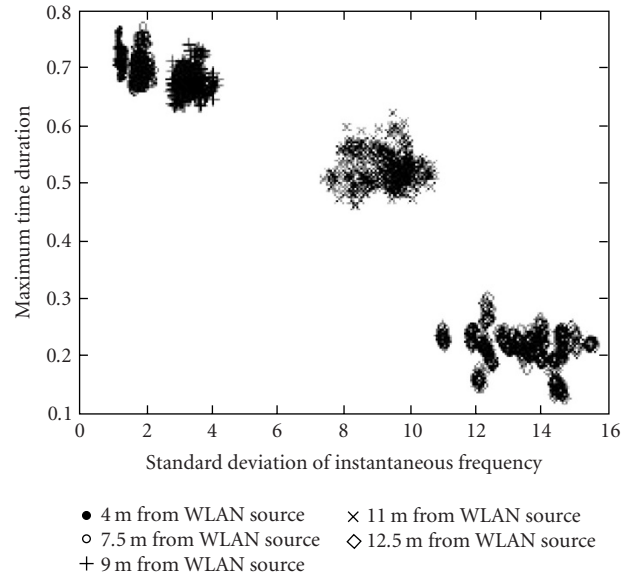


FIGURE 5: Feature plane at multiple-user positions for the WLAN + Bluetooth class by using CW.

The chosen networks are feed forward back-propagation neural networks (FFBPNN) and support vector machines (SVMs). An FFBPNN is trained by the back propagation supervised method [30, 31]. In particular, the learning algorithm is the "batch gradient descent with momentum," so the synaptic weights and biases are updated at the end of the entire training set [14]. Moreover, the momentum version permits one to consider not only the local gradient but also the previous values of the cost function: acting as a low-pass filter, the momentum allows the network to ignore some local minima.

The second classifier, that is, the SVM, has an RBF as kernel, due to the characteristics of the features space, which is composed of nonseparable classes [14, 15]. The equation for the kernel is given by the following formula:

$$K(x_i, x_j) = \exp(-\gamma \cdot \|x_i - x_j\|^2), \quad \gamma > 0. \quad (10)$$

As in the case of this paper, the classical problem of linear SVMs is modified by inserting positive slack variables ξ_i , $i = 1, \dots, l$ [32] to introduce a further cost when necessary. So the constraint that has to be satisfied by the training data becomes

$$y_i \cdot (w^T \phi(x_i) + b) \geq 1 - \xi_i \quad \text{for } \xi_i \geq 0, \quad i = 1, \dots, l. \quad (11)$$

Then the problem of finding the hyperplane is

$$\min_{w, b, \xi} \left\{ \frac{1}{2} w^T w + C \sum_i \xi_i - \sum_i \alpha_i \{y_i (x_i w + b) - 1 + \xi_i\} \right\}, \quad (12)$$

where l is the training set dimension, x_i is the training vector, $y_i \in \{-1, 1\}$ are the training labels, w is the vector normal to the hyperplane, $\phi(x)$ is the mapping function and C is a parameter added to the ξ_i .

TABLE 2: Data of the SVM.

Characteristic	Choi-Williams	Wigner-Ville
Parameters Optimization	Grid search	Grid search
C	16	13777
γ	46.851	18.379
Training vectors	6000	6000

To obtain the best classifier, the parameters have to be optimized. The grid search approach has been chosen to find the values of C and γ (RBF exponent, (10)) and the results are shown in Table 2.

Both classifiers present as input a vector \underline{v} whose components are the features (6) and (8):

$$\underline{v} = [\text{std}(\omega_i), T_M] = [v_1, v_2]. \quad (13)$$

The output is a two-bit variable with one of the four possible values: presence of WLAN (DS-CDMA), presence of Bluetooth (FH-CDMA), presence of both, and presence of noise only.

Having two kinds of TF distributions, two different training vectors for each network have been studied. In particular, the vector \underline{v} is available for the WV transform and is called \underline{v}^W , whereas it is \underline{v}^C for the CW transform.

5. NUMERICAL RESULTS

In this section, results in terms of error classification probability, expressed as relative error frequency, are reported.

For the trials, a power class three [17] for Bluetooth and a 25 mW power level for WLAN are considered [16]. Bit rate equal to 1 Mbps for Bluetooth and 11 Mbps for IEEE 802.11b are used [16, 17]. The number of transmitted bits is equal to 10^4 .

The simulation model of the physical levels of the two standards has been set up in the Matlab/Simulink environment, following all the specifications given by [16, 17], except the presence of coding, which has not been assumed because it is beyond the scope of this paper.

Moreover, a scenario with a single user has been considered: an IEEE 802.11b access point and two Bluetooth picnests are presented. An indoor environment (a $15\text{ m} \times 15\text{ m}$ room) with sources placed in the room corners is considered as described in [33] (see Figure 6). The simulation assumes that a user, provided with an SDR mobile handset, gets into the room where one or both standards are available and have to be identified. The user's movement is simulated straight from the WLAN source to the Bluetooth one [14].

The channel model is a downlink indoor channel at 2.4 GHz. More precisely, a Rician fading channel has been considered with a delay spread of 60 ns and a root mean square (rms) delay spread of 30 ns [34] with AWGN noise. A path loss term has also been added. This term is modeled as described in [33, 35] and introduces an attenuation term

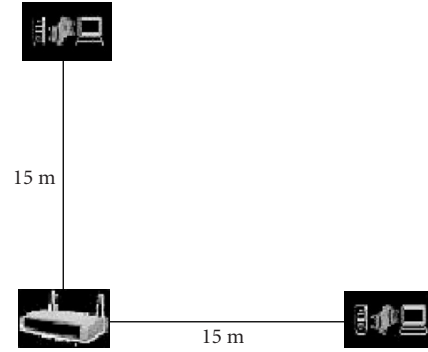


FIGURE 6: Scenario for simulations.

in dB given by

$$L_P = \begin{cases} 32.45 + 20 \log(f \cdot d), & d \leq 8, \\ 58.3 + 33 \log\left(\frac{d}{8}\right), & d > 8, \end{cases} \quad (14)$$

where f is the carrier frequency in GHz and d is the distance in meters from the source. Assuming unitary gains for the transmitter and receiver antennas, the received power P_R is given by

$$P_R = P_T - L_P, \quad (15)$$

where P_T is the transmission power in dB and L_P is the attenuation value (expressed in dB) due to the path loss (14). During the simulations, the signal to noise ratio (SNR) is considered variable with respect to the distance, as the received signal power changes due to the path loss (14)-(15).

Once the signals are passed through the channel, they are converted to IF, and then the A/D conversion is performed at a sample rate of 120 MSample/s to satisfy the Nyquist limit. The IF has been chosen to be equal to 30 MHz. Then the received signal is computed by the TF block.

The WV and CW distributions use blocks with $N = 512$ samples obtained by a time window T long enough to contain 10 frequency hops. The time hopping is $625\ \mu\text{s}$ [16]. The extraction module stores 10 TF matrices and calculates the features as defined in the previous section. The values are passed to the classifiers, which are implemented in the following steps:

- (i) training,
- (ii) testing,
- (iii) evaluation.

Due to the terminal mobility, another critical issue arises: the choice of a significant training vector for the user's movement. This problem has been solved by considering a training set saved at different user positions. This has also been done for the test samples, which have been considered at different points with step shorter than 1 meter to simulate a continuous movement.

TABLE 3: Data of the FFBPNN.

Input	2
Output	2
Levels	4
Neurons for level	5, 5, 4, 2
Activation function	<i>tansig</i>
Epochs	10000
Learning rate	0.1
Goal	0

As reported in Section 4.3, having two possible input vectors, \underline{v}^W and \underline{v}^C (from WV and CW, resp.) and two possible classifiers (FFBPNN and SVM), four configurations have been studied and evaluated:

- (1) FFBPNN with \underline{v}^W ;
- (2) FFBPNN with \underline{v}^C ;
- (3) SVM with \underline{v}^W ;
- (4) SVM with \underline{v}^C .

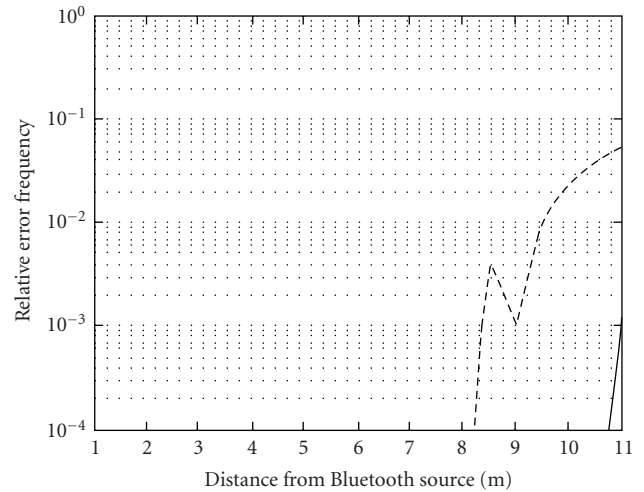
For each configuration, the output of the classifiers is a two-bit variable giving one of the four possible classes (see Section 4.3); the variable represents the mode present in the environment.

The number of levels for the FFBPNN is 4 with 5, 5, 4, and 2 neurons. The activation function is a hyperbolic tangent sigmoid and the learning rate is 10%. The network is trained by means of 1000 different feature vectors presented 10000 times. Other data used for the FFBPNN are given in Table 3.

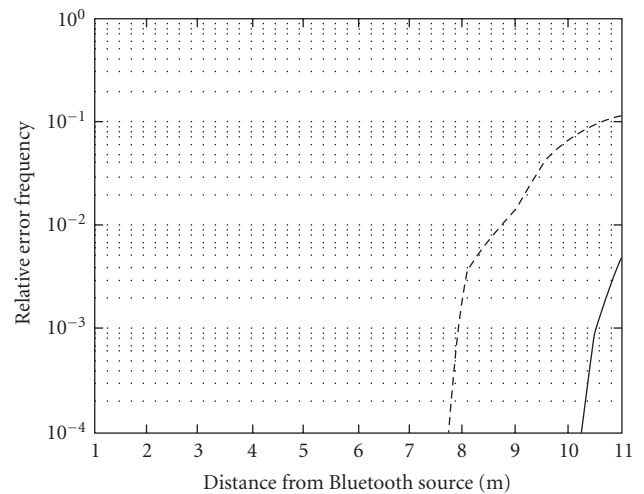
As in the case of the FFBPNN, the SVM has been trained by using two different training vectors (\underline{v}^W and \underline{v}^C), so two different classifiers have been obtained. In Table 2, some parameters of the SVM are presented.

In the following figures, the relative classification error frequency is shown for each class by using the two classifiers and the two TF distributions. The only noise class is always correctly classified. Instead, the case of Bluetooth (BT) classification is depicted in Figures 7a and 7b. In Figure 7a, the SVM classifier shows good performances by the CW distribution, but in the case of WV, some errors occur; the same considerations can be done for the classification by the FFBPNN. The best performances of CW, as compared with the ones of WV results from its behavior with multicomponent signals, like Bluetooth. The CW distribution strongly reduces the so called cross-terms thanks to the exponential kernel, which is not present in the WV distribution.

In Figures 8a and 8b, classification results for the WLAN class are shown. As in previous case, the performances of CW are better than WV. Making a comparison between the two classes, one can notice that the error frequency is higher in the case of WLAN: this is due to the larger overlapping between WLAN and WLAN + Bluetooth than between BT and WLAN + Bluetooth. The superimposition is caused by the higher transmission power of WLAN, which makes the WLAN + Bluetooth class more similar to WLAN than BT, when the user is closer to the sources.



(a)



(b)

FIGURE 7: Relative error frequency of Bluetooth by using (a) the SVM and (b) the FFBPNN.

The results reported above are also demonstrated by Figures 9a and 9b. In this case, the performances of the MI module are good at intermediate distances from both sources. In Figure 9a, the classification using the SVM shows that the WLAN + Bluetooth class is well identified with sufficient error rate values in the range of 3–7 m. But, when the user is closer to one of the sources, $d < 3$ m (closeness of Bluetooth) and $d > 7$ m (closeness of WLAN), the features are very similar to the ones of the nearest source, then the classifiers deduce the presence of only one standard instead of two. Also in this case, best results can be obtained by using CW thanks to its properties, as previously explained.

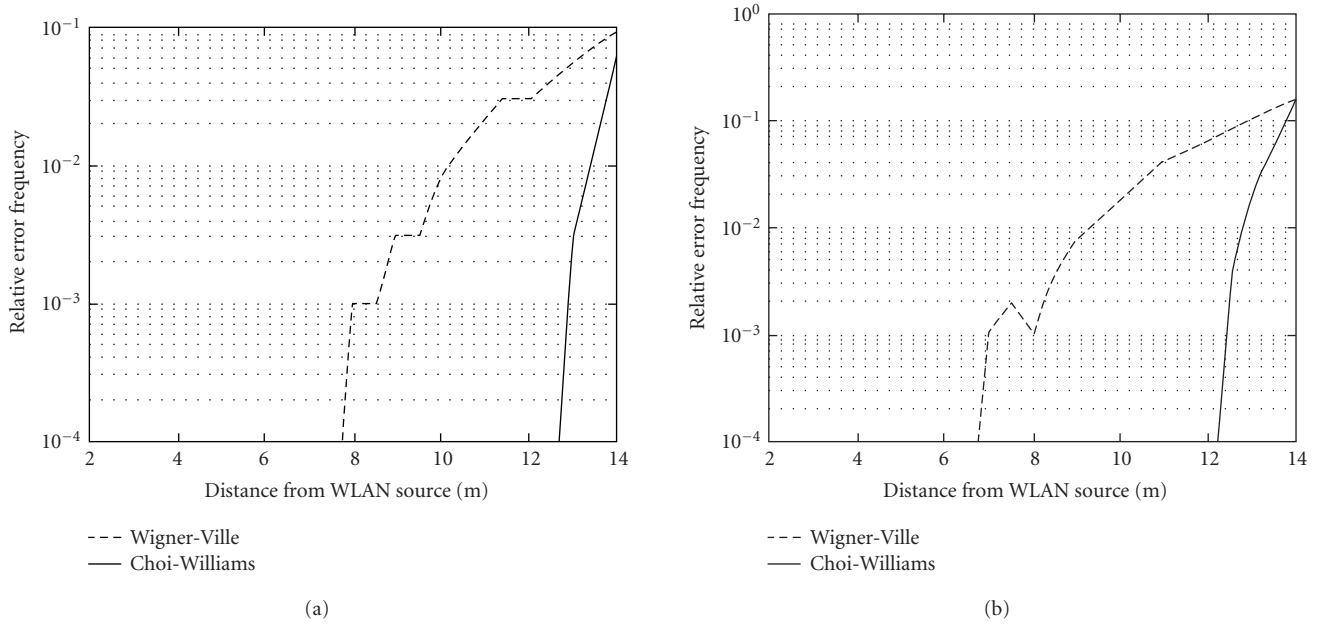


FIGURE 8: Relative error frequency of WLAN by using (a) the SVM and (b) the FFBPNN.

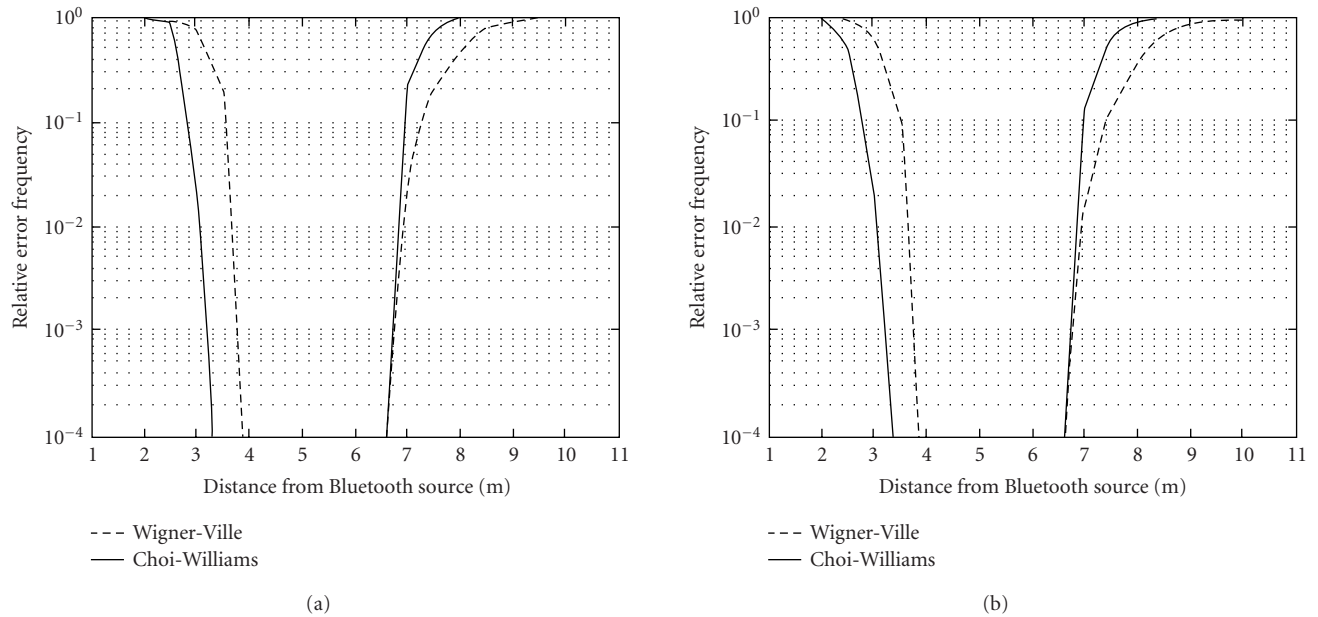


FIGURE 9: Relative error frequency of WLAN + Bluetooth by using (a) the SVM and (b) the FFBPNN.

The behaviors of WLAN + Bluetooth and the other classes can also be found in Table 4, which shows the confusion matrix for a point at 7.5 m from WLAN, using the WV distribution and FFBPNN.

From a TF transform point of view, one can conclude that CW distribution provides better performances than the WV one in all presented cases. As explained, this result stems

from the CW structure, which presents an exponential kernel that strongly reduces auto-interference [13]. The drawback of this transform is a higher computational complexity than that of WV.

Another analysis can be made, considering results plotted for the same distributions but different classifiers. Figures 10a and 10b show a Bluetooth classification by using (a) CW

TABLE 4: Confusion matrix.

Mode	WLAN	Bluetooth	WLAN + Bluetooth	Noise
WLAN	9980	0	20	0
Bluetooth	0	10000	0	0
WLAN + Bluetooth	1290	0	8710	0
Noise	0	0	0	10000

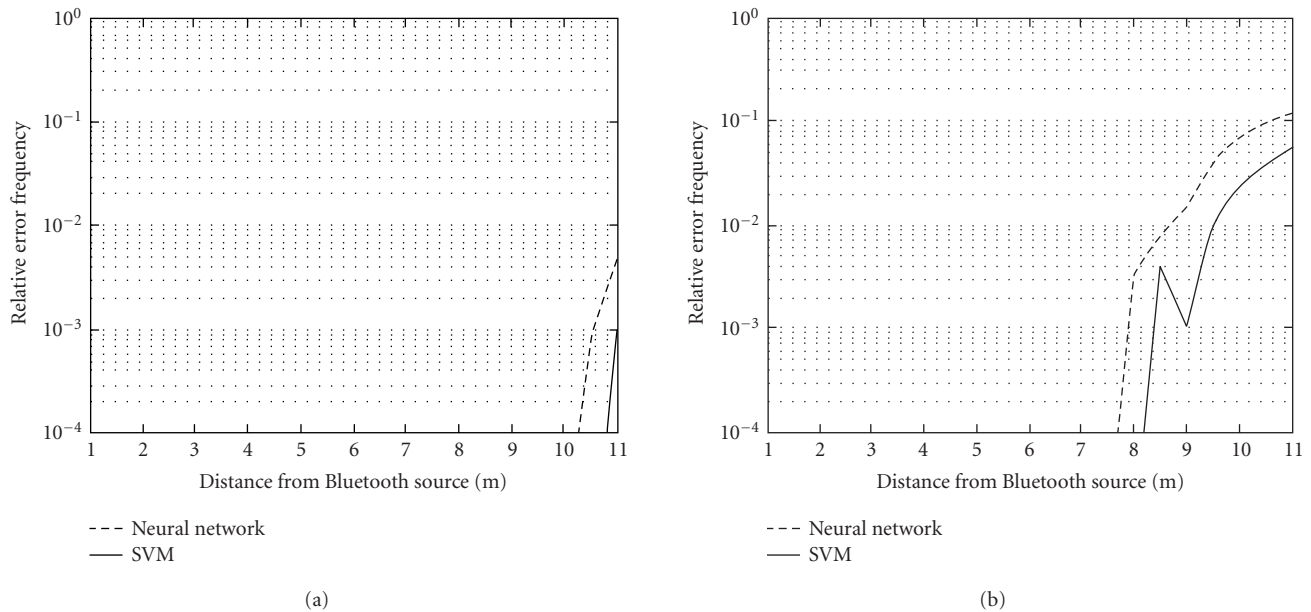


FIGURE 10: Relative error frequency of Bluetooth by using (a) Choi-Williams and (b) Wigner-Ville.

and (b) WV. The results are better for the SVM in both cases thanks to its ability with nonlinear kernels to identify overlapping classes.

6. CONCLUSIONS

In this paper, a method to perform MI for an SDR-based receiver has been proposed and discussed. In particular, attention has been focused on discriminating between two modes (FH-CDMA and DS-CDMA) related to two standards (Bluetooth and IEEE 802.11b) in an indoor environment. TF analysis (by the WV and CW distributions) and neural classifiers (a feedforward network and an SVM) have been proposed as a possible solution. Results in terms of error classification probability (expressed as relative error frequency) with respect to the distances from the sources have been given in the context of a Rician fading download channel in the presence of path loss. The proposed method has yielded good results, which will lead the authors to develop these methodologies by adding new standards and new features. Moreover, the comparisons between the two distributions and the two classifiers point out that the CW distribution and the SVM provide best classification performances. The drawback of this solution is a higher computation load due to the TF distribu-

ACKNOWLEDGMENTS

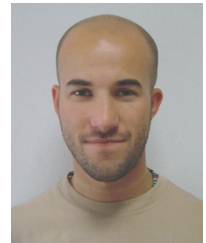
This work was partially developed within the project Virtual Immersive COMMunication (VICOM) funded by the Italian Ministry of University and Scientific Research (FIRB Project). The authors wish to thank the anonymous reviewers for their constructive comments and analyses and Francesco Pantisano for his valuable help in the collection of the paper results.

REFERENCES

- [1] J. Mitola, *Software Radio Architecture: Object-Oriented Approaches to Wireless Systems Engineering*. John Wiley & Sons, New York, NY, USA, 2000.
- [2] T. Turetli and D. Tennenhouse, "Complexity of a software GSM base station," *IEEE Communications Magazine*, vol. 37, no. 2, pp. 113–117, 1999.
- [3] S. Mirabbasi and K. Martin, "Classical and modern receiver architectures," *IEEE Communications Magazine*, vol. 38, no. 11, pp. 132–139, 2000.
- [4] E. Buracchini, "The software radio concept," *IEEE Communications Magazine*, vol. 38, no. 9, pp. 138–143, 2000.
- [5] R. H. Walden, "Performance trends for analog to digital converters," *IEEE Communications Magazine*, vol. 37, no. 2, pp. 96–101, 1999.

- [6] R. D. Murch and K. B. Letaief, "Antenna systems for broadband wireless access," *IEEE Communications Magazine*, vol. 40, no. 4, pp. 76–83, 2002.
- [7] M. Laddomada, F. Daneshgaran, M. Mondin, and R. M. Hickling, "A PC-based software receiver using a novel front-end technology," *IEEE Communications Magazine*, vol. 39, no. 8, pp. 136–145, 2001.
- [8] J. Mitola, *Cognitive radio: an integrated agent architecture for software defined radio*, Ph.D. Dissertation, Department of Teleinformatics Electrum 204, Royal Institute of Technology (KTH), Stockholm, Sweden, May 2000.
- [9] J. Mitola and G. Q. Maguire Jr., "Cognitive radio: making software radios more personal," *IEEE Personal Communications*, vol. 6, no. 4, pp. 13–18, 1999.
- [10] M. Mehta, N. Drew, G. Vardoulas, N. Greco, and C. Niedermeier, "Reconfigurable terminals: an overview of architectural solutions," *IEEE Communications Magazine*, vol. 39, no. 8, pp. 82–89, 2001.
- [11] H. Urkowitz, "Energy Detection of unknown deterministic signals," *Proceedings of IEEE*, vol. 55, no. 4, pp. 523–531, 1967.
- [12] C. Roland and J. Palicot, "A self-adaptive universal receiver," *Annales des Télécommunications*, vol. 57, no. 5-6, pp. 421–456, 2002.
- [13] L. Cohen, *Time-Frequency Analysis*, Prentice-Hall, Englewood Cliffs, NJ, USA, 1995.
- [14] S. Haykin, *Neural Networks: A Comprehensive Foundation*, Prentice-Hall, Upper Saddle River, NJ, USA, 1999.
- [15] N. Cristianini and J. Shawe-Taylor, *An Introduction to Support Vector Machines and Other Kernel-Based Learning Methods*, Cambridge University Press, Cambridge, UK, 2000.
- [16] IEEE 802.11b, "Wireless LAN MAC and PHY specifications: higher speed physical layer (PHY) extension in the 2.4 GHz band," 1999, supplement to 802.11.
- [17] Bluetooth standard, "Specification of the Bluetooth System," volume 1, www.bluetooth.com.
- [18] J. M. Peha, "Wireless communications and coexistence for smart environments," *IEEE Personal Communications*, vol. 7, no. 5, pp. 66–68, 2000.
- [19] P. J. Loughlin, Ed., "Special Issue on Time Frequency Analysis," *Proceedings of the IEEE*, vol. 84, no. 9, 1996.
- [20] N. Golmie, N. Chevrollier, and O. Rebala, "Bluetooth and WLAN coexistence: challenges and solutions," *IEEE Wireless Communications*, vol. 10, no. 6, pp. 22–29, 2003.
- [21] B. Boashash and P. Black, "An efficient real-time implementation of the Wigner-Ville distribution," *IEEE Trans. Acoustics, Speech, and Signal Processing*, vol. 35, no. 11, pp. 1611–1618, 1987.
- [22] G. S. Cunningham and W. J. Williams, "Fast implementations of generalized discrete time-frequency distributions," *IEEE Trans. Signal Processing*, vol. 42, no. 6, pp. 1496–1508, 1994.
- [23] I. Gertner and M. Shamash, "VLSI structures for computing the Wigner distribution," in *Proc. IEEE Int. Conf. Acoustics, Speech, Signal Processing (ICASSP '88)*, vol. 4, pp. 2132–2135, New York, NY, USA, April 1988.
- [24] A. K. Ozdemir and O. Arikan, "Fast computation of the ambiguity function and the Wigner distribution on arbitrary line segments," *IEEE Trans. Signal Processing*, vol. 49, no. 2, pp. 381–393, 2001.
- [25] H. M. Ozaktas, O. Arikan, M. A. Kutay, and G. Bozdogat, "Digital computation of the fractional Fourier transform," *IEEE Trans. Signal Processing*, vol. 44, no. 9, pp. 2141–2150, 1996.
- [26] S. Stankovic and L. Stankovic, "An architecture for the realization of a system for time-frequency signal analysis," *IEEE Transactions on Circuits and Systems II: Analog and Digital Signal Processing*, vol. 44, no. 7, pp. 600–604, 1997.
- [27] H.-I. Choi and W. J. Williams, "Improved time-frequency representation of multicomponent signals using exponential kernels," *IEEE Trans. Acoustics, Speech, and Signal Processing*, vol. 37, no. 6, pp. 862–871, 1989.
- [28] P. J. Loughlin and K. L. Davidson, "Modified Cohen-Lee time-frequency distributions and instantaneous bandwidth of multicomponent signals," *IEEE Trans. Signal Processing*, vol. 49, no. 6, pp. 1153–1165, 2001.
- [29] A. J. E. M. Janssen, "On the locus and spread of pseudo-density functions in the time-frequency plane," *Philips Journal of Research*, vol. 37, no. 3, pp. 79–110, 1982.
- [30] D. E. Rumelhart, G. E. Hinton, and R. J. Williams, "Learning representations by back-propagation errors," *Nature*, vol. 323, pp. 533–536, 1986.
- [31] B. Hassibi and T. Kailath, "Optimal training algorithms and their relation to backpropagation," in *Advances in Neural Information Processing Systems (NIPS '94)*, vol. 7, pp. 191–198, Denver, Colo, USA, November–December 1994.
- [32] C. Cortes and V. Vapnik, "Support-vector networks," *Machine Learning*, vol. 20, no. 3, pp. 273–297, 1995.
- [33] A. Kamerman, *Coexistence between Bluetooth and IEEE 802.11 CCK Solutions to Avoid Mutual Interference*, Lucent Technologies Bell Laboratories, Murray Hill, NJ, USA, January 1999.
- [34] T. A. Wysocki and H.-J. Zepernick, "Characterization of the indoor radio propagation channel at 2.4 GHz," *Journal of Telecommunications and Information Technology*, vol. 1, no. 3-4, pp. 84–90, 2000.
- [35] N. Golmie, R. E. Van Dyck, and A. Soltanian, "Interference of bluetooth and IEEE 802.11: simulation modeling and performance evaluation," in *Proc. 4th International ACM Workshop on Modeling, Analysis and Simulation of Wireless and Mobile Systems*, Rome, Italy, July 2001.

Matteo Gandetto was born in Alessandria, Italy, in 1976. He received the Laurea degree in telecommunication engineering from the University of Genoa in 2001 with a Master's thesis dealing with multimedia data transmission over RTP protocol. He is currently pursuing a Ph.D. in information and communication technologies in Biophysical and Electronic Engineering Department, University of Genoa. His main research activities are wireless communication with reconfigurable terminals and time-frequency analysis applied in telecommunication. He is a member of the Signal Processing & Telecommunications Group in University of Genoa and of the National Inter-University Consortium for Telecommunications.



Marco Guainazzo is currently a Ph.D. student in science and space engineering at the Department of Biophysical and Electronic Engineering (DIBE), University of Genoa, Italy. He received his M.S. degree in telecommunications engineering in 2001. In 2001, he collaborated with the National Inter-University Consortium for Telecommunications (CNIT) on the "Agenzia Spaziale Italiana (ASI)" cofunded research project related to the design of a software-defined radio-based modem for satellite transmissions. Since 2002, he is collaborating with CNIT on the Virtual Immersive Communications (VICom) research project working on the design of mode identification strategies for reconfigurable software-defined radio-based terminal. His research interests are in mode identification algorithms for software-defined radio platform in a single and multiuser scenario.



Carlo S. Regazzoni is Associate Professor of telecommunications at the Department of Biophysical and Electronic Engineering (DIBE) of the University of Genoa. He obtained the Laurea degree and the Ph.D. in telecommunications and signal processing in 1987 and 1992, respectively. He is member of the CNIT Research Unit of Genoa and responsible of the Signal Processing and Telecommunications Group at DIBE. He has been scientific and technical responsible for the R&D activities related to various EU projects, as well as of DIBE participation to several Italian CNR projects, and to industrial research contracts. His main interests concern video sequence processing, understanding, and communications. Professor Regazzoni has been coeditor of three Kluwer books in video surveillance and Guest Editor of two special issues on the same topic on international journal (the proceedings of the IEEE, real time imaging). He has chaired special sessions at international conferences (ICIAP, Eusipco) and he has organized three international workshops in this research field (AVSS 1998, 2001, 2003). He has been invited at IEEE ICIP01 to hold a tutorial on video surveillance. He is author and coauthor of 43 papers in international scientific journals and more than 130 papers in international conferences.

